ERDC/ITL TR-12-5

Information Technology Laboratory

US Army Corps
of Engineers®
Engineer Research and
Development Center

Capacity Verification for Modifying Little Sunflower Flood Control Drainage Structure Stop Log

Guillermo A. Riveros, DeAnna Dixon, and Elias Arredondo

December 2012

ERDC/ITL TR-12-5
December 2012

Capacity Verification for Modifying Little Sunflower Flood Control Drainage Structure Stop Log

Guillermo A. Riveros, DeAnna Dixon, and Elias Arredondo

Information Technology Laboratory
U.S. Army Engineer Research and Development Center
3909 Halls Ferry Road
Vicksburg, MS 39180-6199

Final report

Prepared for U.S. Army Engineer District, Vicksburg
4155 Clay Street, Vicksburg, MS 39183

Under Work Unit 9K76D4

Abstract

The Steel Bayou and Little Sunflower Flood Control Drainage Structures are the two drainage structures of the Yazoo Backwater Project. They were completed in 1969 and 1975, respectively. The structures allow the storm water of the Mississippi Delta to pass through the open vertical lift gates into the Mississippi/Yazoo River when stages on the riverside of the levees are lower than the stages on the interior basin. When the stages of the Mississippi/Yazoo River are higher than the stages of the interior basin, the vertical lift gates are closed, keeping floodwaters from backing up into the South Delta. The Steel Bayou Drainage Structure is located 0.75 mile north of the Yazoo River mile 9.7 and has four vertical lift gates 23.5 ft high and 31 ft wide. The Little Sunflower Drainage Structure is located north of the Yazoo River at mile 32.6 and has two vertical lift gates 25 ft wide and 22.5 ft high.

This report presents analytical and numerical calculations for the modification of the Steel Bayou stop logs to be used permanently at the Little Sunflower project. The calculations were conducted using the approach used to design miter gate horizontal girders using the 2001 criteria of the American Institute of Steel Construction (AISC) and the box girder calculations from the American Association of State Highways and Transportation Officials (AASHTO) Load and Resistance Factor Design (LRFD) bridge manual.

The AISC criteria yielded a cross section capable of resisting 6323.8 psf (101.3 ft of head) while the AASHTO bridge manual determined the weakest section with a capacity of 5229.2 psf (83.8 ft. of head). The numerical investigation correlated well with the box girder calculations and shows that the welding needs to have a capacity of at least the yield strength of the material.

Contents

Figures and Tables

Figures

Tables

Preface

This research was conducted under the Navigation Systems Research Program, Work Unit 9K76D4, "Inspection and Condition Assessment of Steel Hydraulic Structures." Program Manager was James E. Clausner, Associate Technical Director, Coastal and Hydraulics Laboratory (CHL), U.S. Army Engineer Research and Development Center (ERDC), Vicksburg, MS.

This report was prepared by Dr. Guillermo A. Riveros, DeAnna Dixon, and Elias Arredondo, Information Technology Laboratory (ITL), ERDC. The report was prepared under the general supervision of Dr. Kevin Abraham, Acting Chief, Computational Analysis Branch, Computational Science and Engineering Division, ITL; Dr. Robert Wallace, Chief, Computational Science and Engineering Division, ITL; and Dr. Reed Mosher, Director, ITL.

At the time of the publication of this report, COL Kevin J. Wilson was Commander and Executive Director of ERDC. Dr. Jeffery P. Holland was Director.

Unit Conversion Factors

Multiply	By	To Obtain
cubic inches	1.6387064 E-05	cubic meters
feet	0.3048	meters
foot-kips	1.3558	kilonewton-meters
inch-kips	0.11298	kilonewton-meters
inches	0.0254	meters
kips (1,000 lbf)	4,448.222	newtons
kips per square inch	6.894757	megapascals
miles (U.S. statute)	1,609.347	meters
pounds (force)	4.448222	newtons
pounds (force) per inch	175.1268	newtons per meter
pounds (force) per square foot	47.88026	pascals
pounds (force) per square inch	6.894757	kilopascals
pounds (mass) per cubic foot	16.0186	kilograms per cubic meter
square inches	6.4516 E-04	square meters

Notation

a	clear distance between transverse stiffeners, in.
a_r	ratio of web area A_w to cross-sectional area A_f of compression flange, in.^{2}
A	area, in.^{2}
A_c	area of the compression flange, in.^{2}
A_{f_c}	compression flange area, in.^{2}
A_{f_t}	tension flange area, in.^{2}
A_o	enclosed area within the box section, in.^{2}
A_w	web area, in.^{2}
b	width, in.
b_e	effective width, in.
b_f	width of flange, in.
b_{f_c}	width of compression flange, in.
b_{f_t}	width of tension flange, in.
C	ratio of the shear buckling stress to the shear yield strength
C_b	factor to account for moment gradient in beam strength
C_{pg}	slenderness ratio limit

d	perpendicular distance between the centroidal X-X axis and the parallel Y-Y axis of each section
d_o	stiffener spacing, in.
D_c	depth of the web, in.
E	modulus of elasticity, psi
f_c	stress in the compression flange caused by the factored loading under investigation, ksi
f_u	maximum flange stress in the panel under consideration due to the factor loading, ksi
f_v	maximum St. Venant torsional shear stress in the flange plate due to the factored loads, ksi
F_{cr}	critical compression flange stress, ksi
F_n	nominal flexural resistance, ksi
F_r	factored flexural resistance, ksi
F_y	yield stress, ksi
F_{yf}	specified minimum yield strength of the flange, ksi
F_{yw}	yield strength of the web, ksi
F_{yt}	yield stress of tension flange, ksi.
h	distance between flanges when welds are used, in.; maximum height of stop log (Equation 30); height, in. (Tables 2, 4, 6, and 8)
h_c	twice the distance from the section centroid to the inside faces of the flanges when welds are used for built-up sections
$I_{x,c}, I_{y,c}$	moment of inertia about the centroidal x- and y-axis

I_{xx},I_{yy}	moment of inertia about the new xx- and yy-axis
J	torsional constant
k_c	coefficient in $\lambda_r$for welded I-shape
k_v	elastic buckling coefficient for shear strength
K	elastic buckling coefficient for shear strength
L	length of stop log, ft
L_b	laterally unbraced length, in.
M	moment, ft-kips
M_n	nominal flexural strength, ft-kips
M_u	design flexural strength, ft-kips
P_c	maximum pressure, lb/ft^2
r_t	radius of gyration of compression flange plus one-third of the compression portion of the web, in.
r_x,r_y	radius of gyration about the strong and weak axes, respectively
R	weld capacity, kips
R_b	flange-stress reduction factor
R_e	1.0000 for nonhybrid girders
R_h	flange-stress reduction factor = 1.0000 for homogeneous sections
R_{pg}	web stress reduction factor

S_{x_c}, S_{x_t}	section modulus of compression and tension flange, in.^{3}, respectively
t	plate thickness, in.
t_f	thickness of flange, in.
t_{f_c}	thickness of compression flange, in.
t_{max}	maximum thickness within the cross section, in.
t_w	web thickness, in.
T	internal torque resulting from the factored loads, k-in.
V	shear, kips
V_n, V_u	nominal and design shear strength, respectively, kips
V_p	plastic shear force, kips
V_r	factored shear resistance, kips
w	uniform load, lb/ft
w_m, w_s	uniform load for moment and shear, lb/ft, respectively
$\overline{x}$	x-coordinate of the centroid, in.
y	length of compression flange, ft
$\overline{y}$	y-coordinate of the centroid, in.
γ	specific weight of water, lb/ft^3
λ	slenderness ratio limit
λ_p, λ_r	slenderness ratio limit
τ_{max}	maximum shear, kips

φ resistance factor = 0.9000

φ_f resistance factor for flexure = 1.0000

φ_v resistance factor = 0.9000

1 Introduction

The Steel Bayou and Little Sunflower Flood Control Drainage Structures are the two drainage structures of the Yazoo Backwater Project. They were completed in 1969 and 1975, respectively. The structures allow the storm water of the Mississippi Delta to pass through the open vertical lift gates into the Mississippi/Yazoo River when stages on the riverside of the levees are lower than the stages on the interior basin. When the stages of the Mississippi/ Yazoo River are higher than the stages of the interior basin, the vertical lift gates are closed, keeping floodwaters from backing up into the South Delta. The Steel Bayou Drainage Structure is located 0.75 mile[1] north of the Yazoo River mile 9.7 (Figure 1). It has four structural vertical lift gates 23.5 ft high and 31 ft wide as shown in Figures 2 and 3. The Little Sunflower Drainage Structure is located north of the Yazoo River at mile 32.6 (Figure 4). It has two vertical lift gates 25 ft wide and 22.5 ft high as shown in Figures 5 and 6.

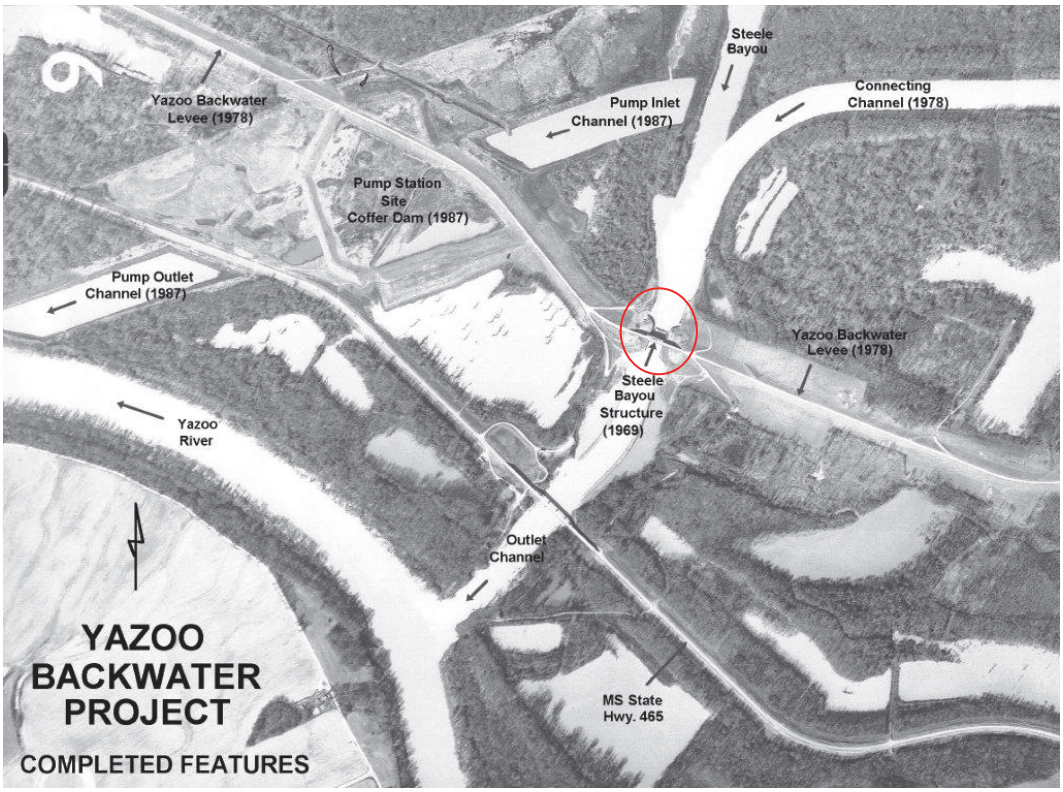

Figure 1. Aerial view of the Steel Bayou Drainage Structure. (Furnished by U.S. Army Engineer District, Vicksburg).

[1] A table of factors for converting non-SI units of measure to SI (metric) units is found on page vii.

Figure 2. The Steel Bayou Flood Control Drainage Structure (photograph reproduced with permission by Quinta Scott, "Steele Bayou Drainage Structure," http://quintascott.wordpress.com, posted on May 31, 2011,accessed 8 May 2012).

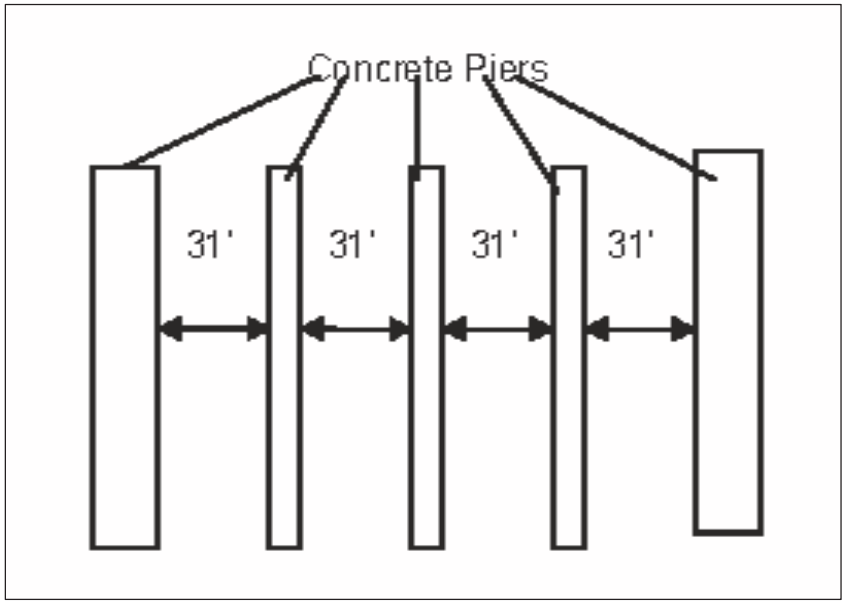

Figure 3. Steel Bayou Drainage Structure: schematic drawing of the width of each vertical lift gate showing the stop logs set between.

Figure 4. Aerial view of the Little Sunflower Drainage Structure.

Figure 5. The Little Sunflower Flood Control Drainage Structure (from Mississippi Levee Board 2012).

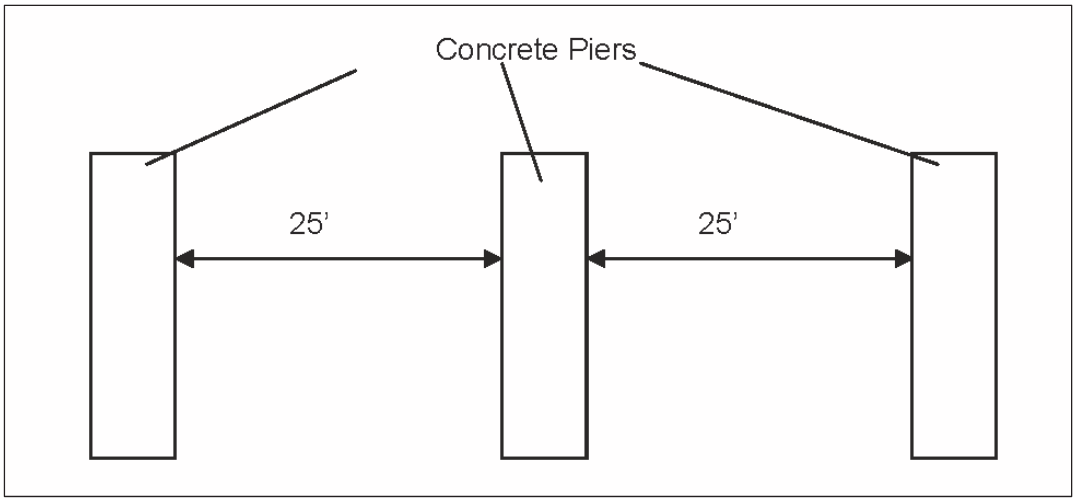

Figure 6. Schematic drawing of the Little Sunflower Drainage Structure showing the width of each vertical lift gate with the stop logs set between

The U.S. Army Engineer District (USAED), Vicksburg, has a set of stop logs that were modified some time ago to be shared between the two structures. They were originally built for the Steel Bayou drainage structures. The Vicksburg District has developed an extension of the stop log (Figure 7). The extension consists of the cross section of the original stop log; however, they are connected with a bolted connection (Figure 8) to obtain the appropriate width and strengths for the Little Sunflower drainage structure. The USAED, Vicksburg, District Operations Division wants to modify the stop logs to be used permanently at the Little Sunflower site. This task will require that a new extension be built and welded to the existing stop log.

Objective

The proposed effort includes multiple directions. First, the capacity of the Little Sunflower stop log must be determined with the new geometrical changes and extension. This will require the verification of the maximum applied loads (demand) that will reach the capacity of the weakest cross section. The capacity of the stop log will be determined using the American Institute of Steel Construction (AISC) Load and Resistance Factor Design (LRFD) (2001) and the American Association of State Highways and Transportation Officials (AASHTO) LRFD Bridge Design Specifications manuals (AASHTO 1998).

Figure 7. Stop log extensions used for the Little Sunflower Flood Control Drainage Structure. (Furnished by USAED Vicksburg.)

Figure 8. Stop logs used on the Steel Bayou Flood Control Drainage Structure. (Furnished by USAED Vicksburg).

Approach

The following two approaches will be used:

- The first approach will involve using a plate girder of a modified box girder section according to the AISC LRFD manual (AISC 2001). This approach is similar to that used to design the horizontal girders of a miter gate (Headquarters, U.S. Army Corps of Engineers, 1994) in which an effective width of the skin plate is calculated and the capacity of an I-section is determined.
- The second approach will involve using the box girder capacity calculation according to the AASHTO LRFD Bridge Design Specifications manual (AASHTO 1998). This approach will also determine the capacity of the welded connection assuming a full-penetration groove weld. A three-dimensional finite element analysis of the stop log will be performed to verify the analytical solutions and to determine any possible hot spots in the structural system that cannot be determined using hand calculation analytical solutions.

2 Flexure and Shear Capacity Calculations

Calculations of the flexural and shear capacities were performed for two different cross sections (Figure 9 and 10). The capacity of the modified cross section (Figure 10) was determined using AISC LRFD (AISC 2001). The cross section was modified into an I-shaped beam with skin plate effective widths for slender, noncompact, and compact sections (Figures 11, 12, and 13, respectively). The flexural and shear strength of the original section (Figure 9) was calculated using the AASHTO LRFD bridge design specifications (AASHTO 1998) for box girder sections. The minimum values of moment and shear of the different methods were used to determine the maximum applied loads used to develop the yield strength.

AISC LRFD method for plate girders

Geometrical properties of slender cross section (b_e = 11.7 in.)[1]

The cross section of the plate girder was modified by cutting the original cross section to find the design flexural and shear strength for plate girders according to Appendix G of AISC LRFD (AISC 2001). The section in Figure 11, the effective width of the flange was taken as half of the distance between the webs of the original cross section. This resulted in an effective width of 11.7 in., making the section slender.

When the limit state for flange local buckling is calculated ($\lambda \leq \lambda_p$), this makes the section compact. Therefore, the calculations for the slender section will not be determined.

Geometrical properties for a noncompact cross section (b_e = 11.1)

The cross section of the plate girder was modified (Figure 12) as if we were to cut the original cross section to find the design flexural and shear strength according to Appendix G of AISC LRFD (AISC 2001). The effective width $b_e = 11.1\text{in.}$ was calculated using Table B5.1 of the AISC LRFD manual (AISC 2001).

[1] Symbols and abbreviations are listed and defined in the notation (page ix)

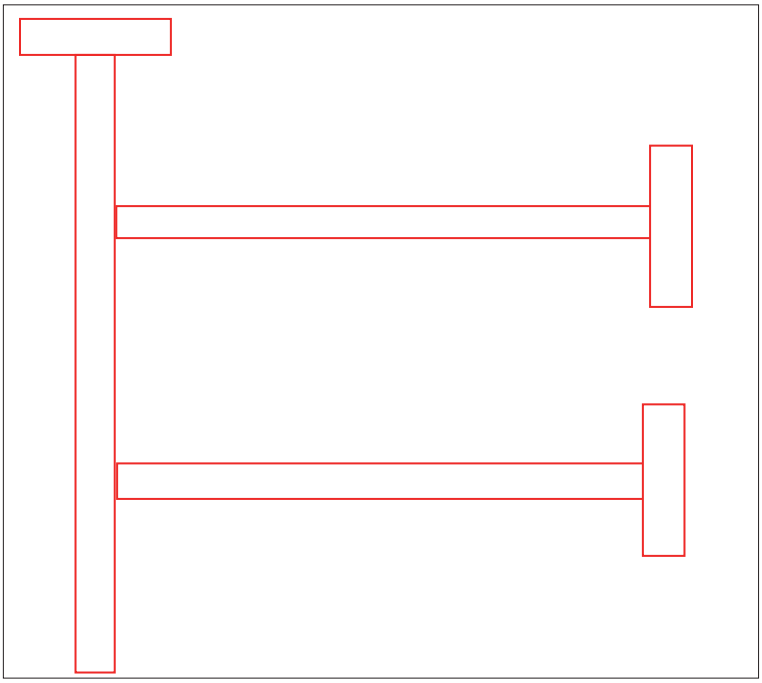

Figure 9. The original cross section used for the AASHTO (1998) LRFD bridge design specification.

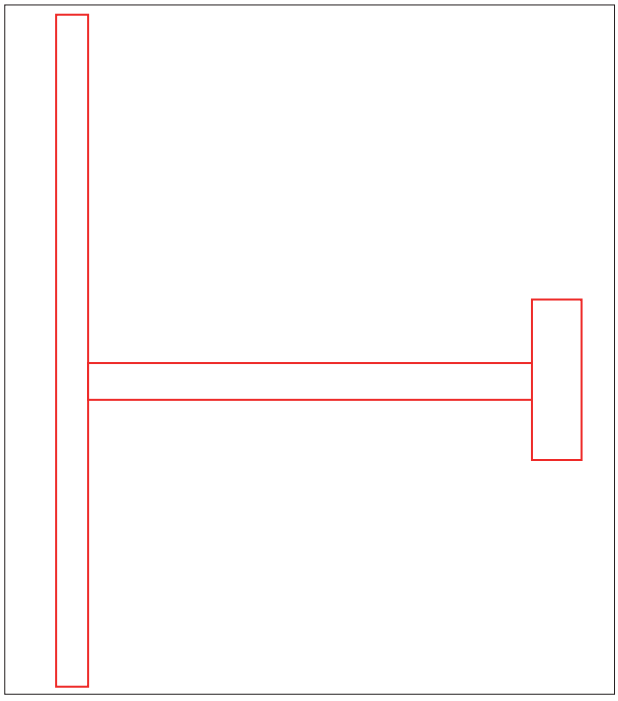

Figure 10. The modified cross section used for the AISC (2001) LRFD method using slender, noncompact, and compact effective widths.

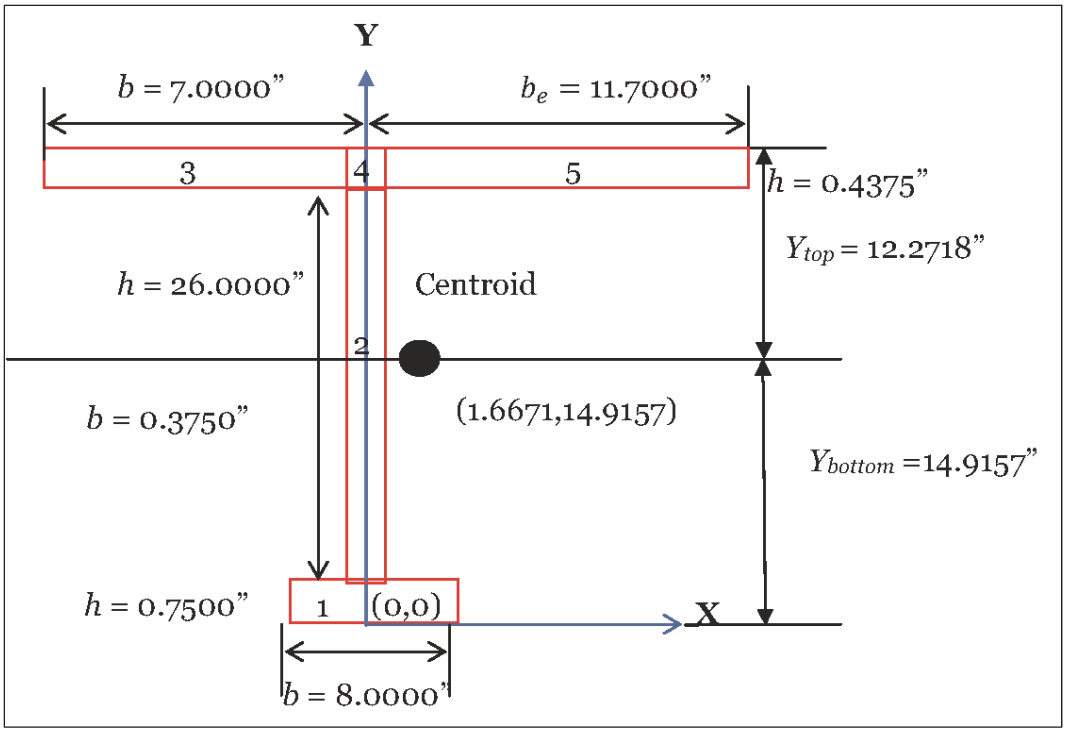

Figure 11. The modified cross section used for the AISC (2001) LRFD method using effective width b_e = 11.7 in. (slender).

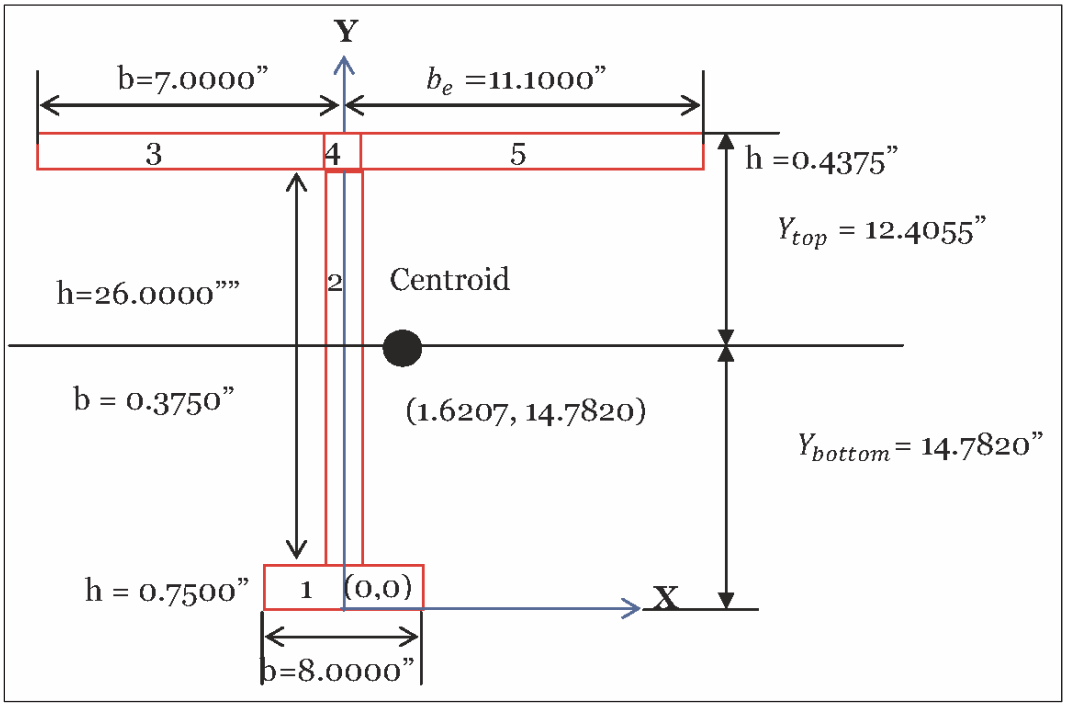

Figure 12. Modified cross section used for the AISC LRFD (AISC 2001) method using effective width b_e = 11.1 in. (noncompact).

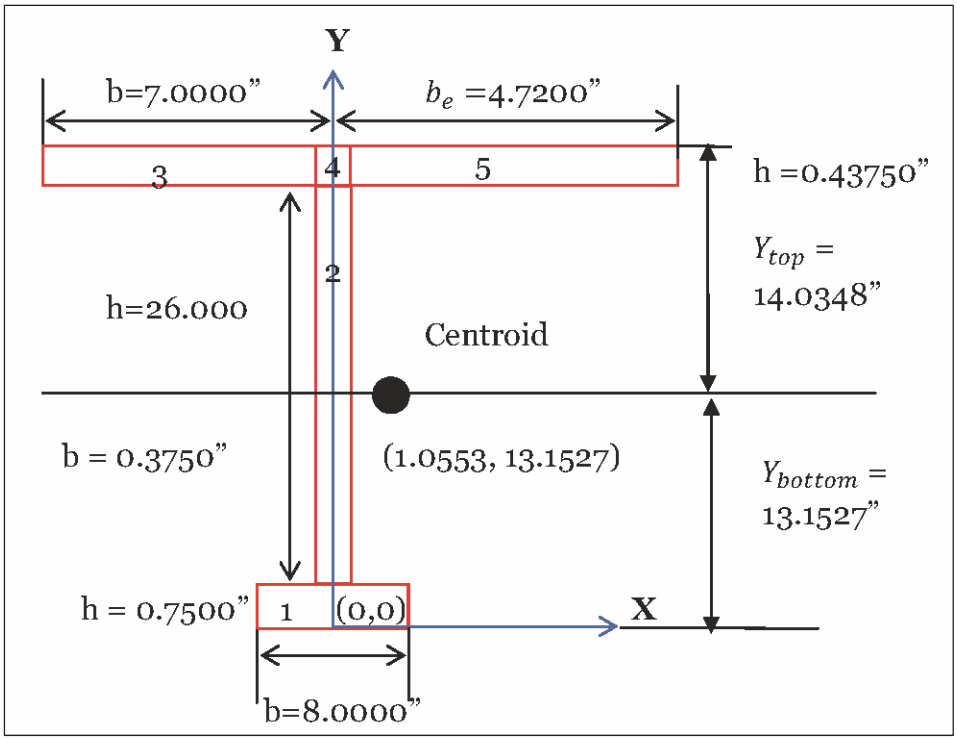

Figure 13. The modified cross section used for the AISC LRFD (AISC 2001) method using effective width b_e = 4.72 in. (compact)

When the limit state for flange local buckling is calculated ($\lambda \leq \lambda_p$), this makes the section compact. Therefore the calculations for the noncompact section will not be determined.

Geometrical properties of a compact cross section (b_e = 4.72)

The cross section of the plate girder was modified (Figure 13) as if the original cross section were to be cut to find the design flexural and shear strength according to Appendix G of AISC LRFD (AISC 2001). The effective width b_e = 4.72 in. was calculated using Table B5.1 of the AISC LRFD manual (AISC 2001).

The y-coordinate of the centroid is calculated as

$$\bar{y} = \frac{\Sigma AY}{\Sigma A} = \frac{274.5977\,in^3}{20.8776\,in^2} = 13.1527\,in. \quad (1)$$

where Y is measured from the base of Figure 13 to the centroid of each section. Table 1 lists the geometrical properties of the cross section in the y-direction for b_e = 4.72 in. (compact).

Table 1. Geometrical properties of the cross section in y-direction for b_e = 4.72 in. (compact).

Section	*b*, in.	*h*, in.	*A*, in.²	*Y*, in.	*AY*, in.³
1	8.0000	0.7500	6.0000	0.3750	2.2500
2	0.3750	26.0000	9.7500	13.7500	134.0625
3	6.8125	0.4375	2.9805	26.9688	80.3805
4	0.3750	0.4375	0.1641	26.9688	4.4256
5	4.5325	0.4375	1.9830	26.9688	53.4791
			Σ=20.8776		Σ=274.5977

Note: *b* = in.; *h* = height, in.; *A* = area, in.²;

The moment of inertia about the new *xx*-axis is calculated as

$$I_{xx} = I_{x,c} + Ad^2 = 2508.2380\,in.^4 \tag{2}$$

where

I_{xx} = moment of inertia about the new *xx*-axis
$I_{x,c,}$ = moment of inertia about the centroidal *x*-axis
d = perpendicular distance between the centroidal *X*-*X* axis and the parallel *Y*-*Y* axis of each section

Table 2 lists the geometrical properties used to determine the moment of inertia in the *y*-direction for b_e = 4.72 in. (compact).

Table 2. Geometrical properties used to determine the moment of inertia in *y*-direction for b_e = 4.72 in. (compact)

Section	$I_{x,c} = \frac{bh^3}{12}$ in.⁴	*A*, in.²	*d*, in.	Ad^2, in.³
1	0.2813	6.0000	12.7777	979.6177
2	549.2500	9.7500	0.1527	0.2273
3	0.0475	2.9805	-13.8161	568.9316
4	0.0026	0.1641	-13.8161	31.3242
5	0.0316	1.9830	-13.8161	378.5242
	Σ=549.6130	Σ=20.8776		Σ=1958.6250

The *x*-coordinate of the centroid is calculated as

$$\bar{x} = \frac{\Sigma AX}{\Sigma A} = \frac{22.0323\,\text{in.}^3}{20.8776\,\text{in.}^2} = 1.0553\,in. \quad (3)$$

where X is measured as the absolute distance from the origin of the X-axis to the center of the base of Figure 13. Table 3 lists the geometrical properties of the cross section in the x-direction for b_e=4.72 in. (compact).

Table 3. Geometrical properties of the cross section in the x-direction for b_e=4.72 in. (compact).

Section	b, in.	h, in.	A, in.^{2}	X, in.	AX, in.^{3}
1	8.0000	0.7500	6.0000	0.0000	0.0000
2	0.3750	26.0000	9.7500	0.0000	0.0000
3	6.8125	0.4375	2.9805	3.5000	10.4318
4	0.3750	0.4375	0.1641	0.0000	0.0000
5	4.5325	0.4375	1.9830	5.8500	11.6005
			Σ=20.8776		Σ=22.0323

The moment of inertia about the new yy-axis is calculated as

$$I_{yy} = I_{y,c} + Ad^2 = 209.9820 in.^4 \quad (4)$$

where

I_{yy} = moment of inertia about the new yy-axis
$I_{y,c}$ = moment of inertia about the centroidal y-axis

Table 4 lists the geometrical properties used to determine the moment of inertia in the x-direction for b_e=4.72 in. (compact)

Table 4. Geometrical properties used to determine the moment of inertia in the x-direction for b_e=4.72 in. (compact).

Section	$I_{y,c} = \frac{b^3 h}{12}$ in.^{4}	A, in.^{4}	d, in.	Ad^2, in.^{4}
1	32.0000	6.0000	1.6671	16.6753
2	0.1143	9.7500	1.6671	27.0974
3	11.5270	2.9805	5.2609	82.4915
4	0.0019	0.1641	1.6671	0.4561
5	3.3948	1.9830	4.2767	36.2237
	Σ=47.0380	Σ=20.8776		Σ=162.9440

Results for the radius of gyration about the strong and weak axes are shown in Equations 5 and 6, respectively. Equations 7 and 8 show the section modulus of tension and compression, respectively, for the strong axis.

$$r_x = \sqrt{\frac{I_{xx}}{A}} = \sqrt{\frac{2508.2380\,in.^4}{20.8776\,in^2}} = 10.9608\,in. \tag{5}$$

$$r_y = \sqrt{\frac{I_{yy}}{A}} = \sqrt{\frac{209.9820\,in.^4}{20.8776\,in.^2}} = 3.1714\,in. \tag{6}$$

$$S_{x_t} = \frac{I_{xx}}{y_{top}} = \frac{2508.2380\,in.^4}{14.0348\,in.} = 178.7156\,in.^3 \tag{7}$$

$$S_{x_c} = \frac{I_{xx}}{y_{bottom}} = \frac{2508.2380\,in.^4}{13.1527\,in.} = 190.7014\,in.^3 \tag{8}$$

where

r_x = radius of gyration about the strong axis, in.
r_y = radius of gyration about the weak axis, in.
S_{x_t} = section modulus of tension flange, in.^{3}
S_{x_c} = section modulus of compression flange, in.^{3}

Calculations of design and shear capacities for compact cross section (b_e = 4.72 in.)

Design flexural strength

The cross section is ASTM-A36 Steel with a modulus of elasticity of $E = 29 \times 10^6\ psi$.

Tension-flange yield

$$M_n = S_{xt} \times R_e \times F_{yt} \tag{9}$$

where

M_n = nominal flexural strength, ft-kips
R_e = 1.0000 for nonhybrid girders

F_{yt} = yield stress of tension flange, ksi

M_n = (178.7156 in.3)(1.0000)(36.0000 ksi) = 6,433.7616 in. – kips = 536.1468 ft – kips

$$M_u = M_n \times \phi \tag{10}$$

where

M_u = design flexural strength, ft-kips

ϕ = resistance factor = 0.9000

M_u = (536.1468 ft – kips)(0.9000) = 482.5321 ft – kips

Compression-flange buckling

$$M_n = S_{xc} \times R_{pg} \times R_e \times F_{cr} \tag{11}$$

where F_{cr} is the critical compression flange stress, ksi.

$$R_{pg} = 1 - \frac{a_r}{1200 + 300a_r}\left(\frac{h_c}{t_w} - 5.70\sqrt{\frac{E}{F_{cr}}}\right) \leq 1.0 \tag{12}$$

$$a_r = \frac{A_w}{A_{fc}} = \frac{2h_c t_w}{b_{fc} t_{fc}} = \frac{2(12.4027\,in.)(0.3750\,in.)}{(8.0000\,in.)(0.7500\,in.)} = 1.5503 \tag{13}$$

where

R_{pg} = web stress reduction factor

a_r = ratio of web area A_w to cross sectional area A_{fc} of compression flange, in.^{2}

h_c = twice the distance from the section centroid to the inside faces of the flanges when welds are used for built-up sections

t_w = web thickness, in.

E = modulus of elasticity, psi

A_w = web area, in.^{2}

A_{fc} = compression flange area, in.^{2}

b_{fc} = width of compression flange, in.

t_{fc} = thickness of compression flange, in.

$$R_{pg} = 1 - \frac{1.5503}{1200 + 300(1.5503)}\left(\frac{12.4027\,in.}{0.3750\,in.} - 5.70\sqrt{\frac{29{,}000\,ksi}{36.000\,ksi}}\right) = 1.1198$$

The critical stress F_{cr} to be used is dependent upon the slenderness parameters $\lambda, \lambda_r, \lambda_p$ and C_{pg} as follows:

1. Limit state of lateral-torsional buckling:

$$\lambda = \frac{L_b}{r_T} = \frac{92.5625\,in.}{0.2165\,in. + 4.1342\,in.} = 21.2753 \tag{14}$$

where

L_b = laterally unbraced length, in. (Figure 14)
r_T = radius of gyration of compression flange plus 1/3 of the compression portion of the web, in.

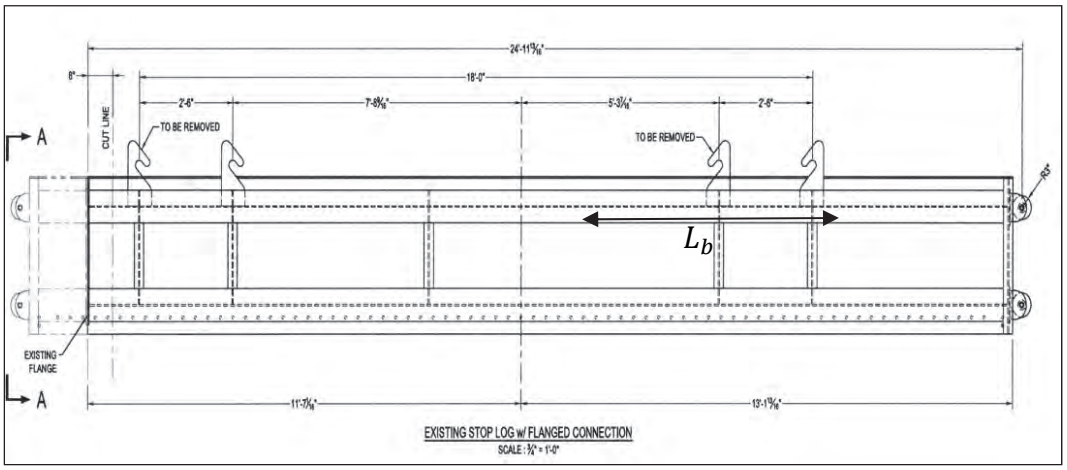

Figure 14. Distance of L_b as it relates to the stop log. (Furnished by USAED, Vicksburg).

$$\lambda_p = 1.76\sqrt{\frac{E}{F_{yf}}} = 49.9529 \tag{15}$$

$$\lambda_r = 4.44\sqrt{\frac{E}{F_{yf}}} = 126.0175 \tag{16}$$

$$\text{For } \lambda \le \lambda_p \text{, then } F_{cr} = F_{yf}$$

where F_{yf} is the specified minimum yield strength of the flange, ksi.

$$\begin{aligned} M_n &= S_{xc} \times R_{pg} \times R_e \times F_{cr} \\ &= \left(190.7014\, in.^3\right)\left(1.1198\right)\left(1.0000\right)\left(36.0000\, ksi\right) \\ &= 7{,}687.7074\, in.-kips = 640.6423\ ft-kips \end{aligned}$$

$$M_u = M_n \times \phi = \left(640.6423\ ft-kips\right)\left(0.9000\right) = 576.5780\ ft-kips$$

2. Limit state of flange local buckling:

$$\lambda = \frac{b_f}{t_f} = \frac{8.0000\, in.}{\left(0.7500\, in.\right)} = 10.6667 \tag{17}$$

where b_f and t_f are the width and thickness of the flange, in., respectively.

$$\lambda_p = 0.38\sqrt{\frac{E}{F_{yf}}} = 10.7853 \tag{18}$$

$$\lambda_r = 1.35\sqrt{\frac{E}{\frac{F_{yf}}{k_c}}} = 26.5572 \tag{19}$$

where k_c, the coefficient in λ_r for welded I-shape, is calculated as

$$k_c = \frac{4}{\sqrt{\frac{h}{t_w}}} = \frac{4}{\sqrt{\frac{26.0000}{0.3750}}} = 0.4804 \tag{20}$$

For $\lambda \le \lambda_p$ then,

$$F_{cr} = F_{yf} \tag{21}$$

$$R_{pg} = 1 - \frac{1.5503}{1200 + 300\left(1.5503\right)}\left(\frac{12.4027\, in.}{0.3750\, in.} - 5.70\sqrt{\frac{29{,}000\, ksi}{36.0000\, ksi}}\right) = 1.1198$$

$$M_n = S_{xc} \times R_{pg} \times R_e \times F_{cr}$$
$$= (190.7014)(1.1198)(1.000)(36.000\,ksi)$$
$$= 7687.7074\,in.-kips = 640.6423\ ft-kips$$

$$M_u = M_n \times \phi = (640.6423\ ft-kips)(0.9000) = 576.5781\ ft-kips$$

Design shear strength

According to Section G3.1 of AISC (2010), consideration for tension field action is not permitted for the following:

- For end panels in all members with transverse stiffeners;
- When $\frac{a}{h}$ exceeds 3.0 or $\left[\frac{260}{\left(\frac{h}{t_w}\right)}\right]^2$;
- When $\frac{2A_w}{A_{fc}+A_{ft}} > 2.5$; or
- When $\frac{h}{b_{fc}}$ *or* $\frac{h}{b_{ft}} > 6.0$.

For this case,

$$\frac{a}{h} = \frac{92.5626}{26.000} = 3.5601 > 3$$

where

a = clear distance between transverse stiffeners, in.
A_w = web area, in.^{2}
A_{f_c} = compression flange area, in.^{2}
b_{f_t} = width of tension flange, in.

Therefore, tension field action is not considered.

$$V_u = \phi_v V_n \tag{22}$$

where

V_u = design shear strength, kips
ϕ_v = resistance factor=0.9000

V_n = nominal shear strength, kips

For

$$\text{If } \frac{h}{t_w} \leq 1.10\sqrt{\frac{k_v E}{F_{yw}}}$$

Then,

$$V_n = 0.6 F_{yw} A_w \tag{23}$$

where

k_v = the elastic buckling coefficient for shear strength
F_{yw} = yield strength of the web, ksi

$$k_v = 5.0000$$

$$\text{when } \frac{a}{h} > 3$$

$$\frac{a}{h} = \frac{92.5625}{26.0000} = 3.5601$$

$$\text{therefore, } k_v = 5$$

$$\frac{h}{t_w} = \frac{26.0000}{0.3750} = 69.333\overline{3} \text{ and}$$

$$1.10\sqrt{\frac{k_v E}{F_{yw}}} = 1.10\sqrt{\frac{(5.0000)(29{,}000)}{36}} = 69.8113$$

$$69.333\overline{3} \leq 69.8113$$

Therefore

$$V_n = 0.6 F_{yw} A_w = (0.6000)(36.0000 ksi)(26.0000 in. \times 0.3750 in.)$$
$$= 210.6000 \, kips$$

$$V_u = \phi_v V_n = (210.6000\,kips)(0.9000) = 189.5400\,kips$$

The maximum uniform loads were determined using the minimum moment of 482.6932 ft-kips (tension flange) and a shear capacity of 189.5400 kips calculated using Equations 25 and 27.

$$M = \frac{w_m L^2}{8} \tag{24}$$

where

M = moment (ft-kips)
w_m = uniform load for moment, lb/ft
L = length of stop log (ft)

Equation 24 was modified as follows:

$$w_m = \frac{M \times 8}{L^2} \tag{25}$$

$$w_m = \frac{482.5321\,ft-kips \times 8.0000 \times 1000.0000\,lb}{25.0000^2\ ft^2} = 6176.4109\,lb\ /\ ft$$

$$V = \frac{w_s \times L}{2} \tag{26}$$

where

V = shear (kips)
w_s = uniform load for shear, lb/ft

Equation 26 was modified as follows:

$$w_s = \frac{V \times 2}{L} \tag{27}$$

$$w_s = \frac{189.5400\,kips \times 2.0000 \times 1000.0000\,lb}{25.0000\ ft} = 15{,}163.2000\,lb\ /\ ft$$

The maximum pressure was determined using the minimum uniform load value between the moment and shear.

$$P_c = \frac{w}{y} \tag{28}$$

where

P_c = maximum pressure, lb/ft^2
w = minimum uniform load, lb/ft
y = width of compression flange, ft

$$P_c = \frac{6176.4109\,lb\ /\ ft}{0.9767\ ft} = 6{,}323.7544\,lb\ /\ ft$$

Then, the maximum height of water that the stop log can resist at the moment the yield strength is accomplished is as follows:

$$h = \frac{P_c}{\gamma} \tag{29}$$

where

h = maximum height of stop log, ft
γ = specific weight of water, lb/ft^3

$$h = \frac{6{,}323.7544\,lb\ /\ ft\ \frac{lb}{ft^2}}{62.4000\,\frac{lb}{ft^3}} = 101.3422\ ft$$

AASHTO LRFD method for single box sections

Geometrical properties of box girder cross section

The following cross section was used to find the design flexural and shear strength according to AASHTO LRFD Bridge Specification Section 6.11.2 (AASHTO 1998) for box sections.

The geometrical properties were calculated by dividing the section (Figure 15) into eight parts. The results for the Y-Y neutral axis and the

moment of inertia on X-X are shown in Tables 5 and 6, while the results for the X-X neutral axis and the moment of inertia on Y-Y are shown in Tables 7 and 8.

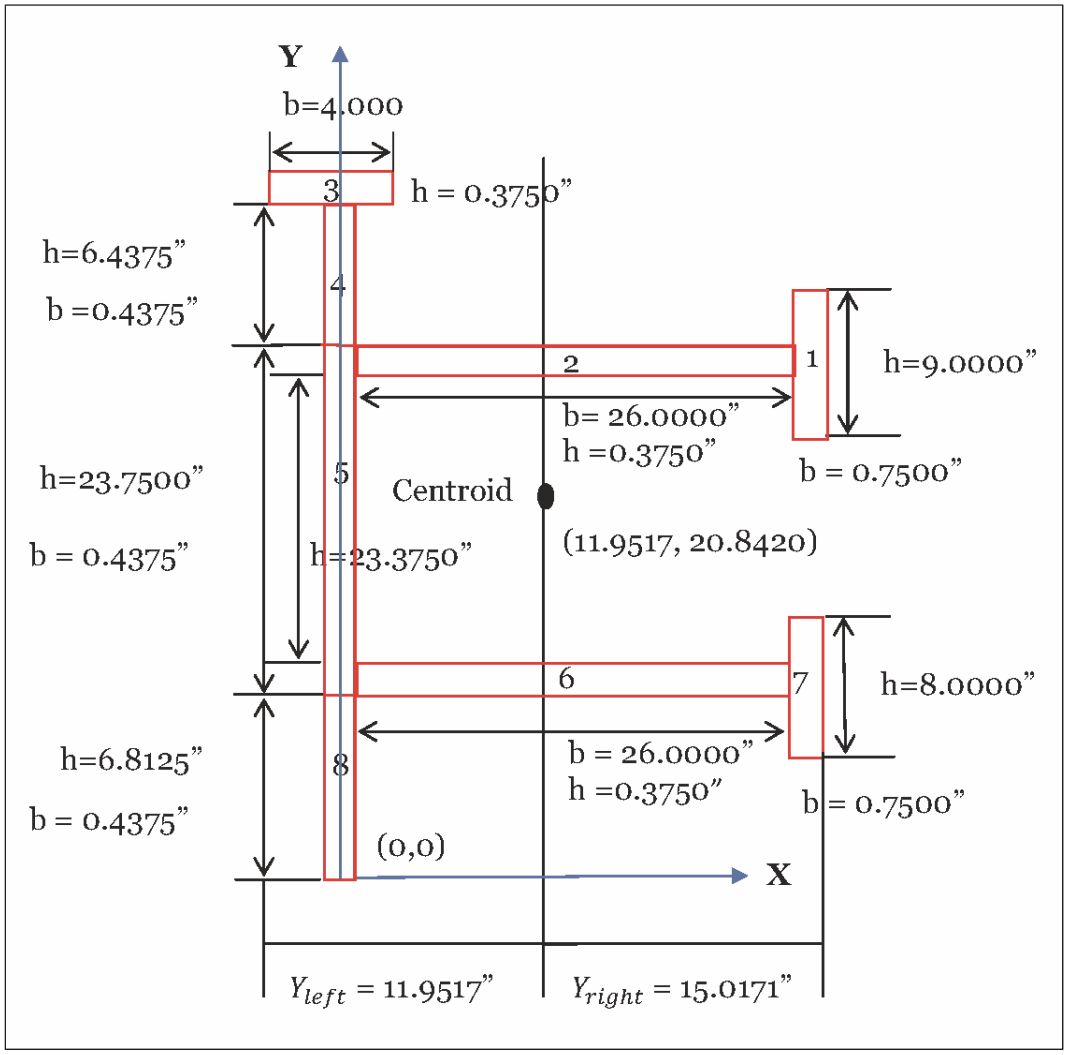

Figure 15. Original cross section used for the AASHTO (1998) LRFD bridge design specification.

Table 5. Geometrical properties of the cross section in *y*-direction for box girders.

Section	*b*, in.	*h*, in.	*A*, in.^{2}	Y, in.	*AY*, in.^{3}
1	0.7500	9.0000	6.7500	34.6875	234.1406
2	26.0000	0.3750	9.7500	34.6875	338.2031
3	4.0000	0.3750	1.5000	37.1875	55.7813
4	0.4375	6.4375	2.8164	33.7813	95.1417
5	0.4375	23.7500	10.3906	18.6875	194.1743
6	26.0000	0.3750	9.7500	7.1875	70.0781

7	0.7500	8.0000	6.0000	7.1875	43.1250
8	0.4375	6.8125	2.9805	3.4063	10.1525
			Σ=49.9375		Σ=1040.7966

Table 6. Geometrical properties used to determine the moment of inertia in *y*-direction of box girders.

Section	$I_{x,c} = bh^3/12$ in.^{4}	*A*, in.^{2}	*d*, in,	Ad^2, in.^{4}
1	45.5625	6.7500	9.3455	589.5340
2	0.1143	9.7500	9.3455	851.5491
3	0.0176	1.5000	16.3455	400.7631
4	9.7263	2.8164	12.9393	471.5371
5	488.4135	10.3906	-2.1545	48.2318
6	0.1143	9.7500	13.6545	1817.8424
7	32.0000	6.0000	13.6545	1118.6722
8	11.5270	2.9805	17.4357	906.0828
	Σ = 587.4755	Σ=49.9375		Σ=6204.2125

Table 7. Geometrical properties of the cross section in *x*-direction for box girders.

Section	*b*, in.	*h*, in.	*A*, in.^{2}	*X*, in.	*AX*, in^3
1	0.7500	9.0000	6.7500	26.5938	179.5082
2	26.0000	0.3750	9.7500	13.2188	128.8833
3	4.0000	0.3750	1.5000	0.0000	0.0000
4	0.4375	6.4375	2.8164	0.0000	0.0000
5	0.4375	23.7500	10.3906	0.0000	0.0000
6	26.0000	0.3750	9.7500	13.2188	128.8833
7	0.7500	8.0000	6.0000	26.5938	159.5628
8	0.4375	6.8125	2.9805	0.0000	0.0000
			Σ = 49.9375		Σ = 596.8376

Table 8. Geometrical properties used to determine the moment of inertia in *x*-direction of box girders.

Section	$I_{y,c} = b^3h/12$ in.^{4}	*A*, in.^{2}	*d*,in.	*Ad*^{2}, in.^{4}
1	0.3164	6.7500	14.6421	1447.1399
2	549.2500	9.7500	1.2671	15.6540
3	2.0000	1.5000	11.9517	214.2647
4	0.0449	2.8164	11.9517	402.3034
5	0.1657	10.3906	11.9517	1484.2259

6	549.2500	9.7500	1.2671	15.6540
7	0.2813	6.0000	14.6421	1286.3466
8	0.0475	2.9805	11.9517	425.7440
	Σ = 1101.3558	Σ = 49.9375		Σ=5291.3325

The *y*-coordinate of the centroid is calculated as

$$\bar{y} = \frac{\Sigma AY}{\Sigma A} = \frac{1040.7966\,in.^3}{49.9375\,in.^2} = 20.8420\,in. \quad (30)$$

where *Y* is measured from the base of Figure 15 to the centroid of each section.

The moment of inertia about the new *xx*-axis is calculated as

$$I_{xx} = I_{x,c} + Ad^2 = 6791.6880\,in.^4 \quad (31)$$

where *d* is the perpendicular distance between the centroidal *Y*-*Y* axis and the parallel *X*-*X* axis of each section.

The *x*-coordinate of the centroid is calculated as

$$\bar{x} = \frac{\Sigma AX}{\Sigma A} = \frac{596.8376\,in^3}{49.9375\,in^2} = 11.9517\,in. \quad (32)$$

where *X* is measured as the absolute distance from the origin of the *X*-axis to the center of the base of Figure 15.

The moment of inertia about the new *yy*-axis is calculated as

$$I_{yy} = I_{y,c} + Ad^2 = 6392.6883\,in.^4 \quad (33)$$

where *d* is the perpendicular distance between the centroidal *X*-*X* axis and the parallel *Y*-*Y* axis of each section.

Results for the radius of gyration about the strong and weak axes are shown in Equations 34 and 35, respectively. Equations 36 and 37 show the section modulus of tension and compression, respectively, for the strong axis.

$$r_x = \sqrt{\frac{I_{xx}}{A}} = \sqrt{\frac{6791.6880\,in.^4}{49.9375\,in.^2}} = 11.6621\,in. \tag{34}$$

$$r_y = \sqrt{\frac{I_{yy}}{A}} = \sqrt{\frac{6392.6883\,in.^4}{49.9375\,in.^2}} = 11.313\,in. \tag{35}$$

$$S_{x_t} = \frac{I_{xx}}{y_{left}} = \frac{6791.6880\,in.^4}{11.9517\,in.} = 568.2613\,in.^3 \tag{36}$$

$$S_{x_c} = \frac{I_{xx}}{y_{right}} = \frac{6791.6880\,in.^4}{15.0171\,in.} = 452.2636\,in.^3 \tag{37}$$

Calculations of the flexural and shear capacities

The cross section is ASTM-A36 Steel and has a modulus of elasticity of $E = 29 \times 10^6\ psi$.

Nominal flexure resistance

$$F_r = \phi_f F_n \tag{38}$$

where

F_r = factored flexural resistance, ksi
ϕ_f = resistance factor for flexure =1.0000
F_n = nominal flexural resistance, ksi

1. Positive Flexure

   (a) Top flange (tension)

$$F_n = R_b R_h F_{yf} \tag{39}$$

where

R_b = flange-stress reduction factor = 1.0000 for tension flanges
R_h = flange-stress reduction factor = 1.0000 for homogeneous sections

$$F_n = R_b R_h F_{yf} = (1.0000)(1.0000)(36.0000\,ksi) = 36.0000\,ksi$$

$$F_r = \phi_f F_n = (1.0000)(36.0000\,ksi) = 36.0000\,ksi$$

$$M = F_r S_{xt} \tag{40}$$

$$M = (36.0000\,ksi)(568.2613\,in.^3) = 20{,}457.4068\,in.-kips = 1{,}704.7839\ ft-kips$$

2. Bottom Flange (Compression)

$$F_n = R_b R_h F_{yf} \sqrt{1 - 3\left(\frac{f_v}{F_{yf}}\right)^2} \tag{41}$$

where f_v is the maximum St. Venant torsional shear stress in the flange plate due to the factored loads, ksi

$$R_b = 1 - \left(\frac{a_r}{1200 + 300 a_r}\right)\left(\frac{2D_c}{t_w} - \lambda_b\sqrt{\frac{E}{f_c}}\right) \tag{42}$$

For which,

$$a_r = \frac{2D_c t_w}{A_c} \tag{43}$$

where

D_c = depth of the web, in.
A_c = area of the compression flange, in.^{2}
λ_b = 4.64 for members with compression flange area less than the tension flange area
f_c = stress in the compression flange due to the factored loading under investigation, ksi

Assume that $f_c = F_{yf}$

$$a_r = \frac{2.0000 \times 26.0000\,in. \times 0.3750\,in.}{(9.0000\,in. \times 0.7500\,in.) + (8.0000\,in. \times 0.7500\,in.)} = 1.5294$$

$$R_b = 1 - \left(\frac{1.5294}{1200 + 300(1.5294)}\right)\left(\frac{2.0000 \times 26.0000\,in.}{0.3750\,in.} - 4.64\sqrt{\frac{29{,}000\,ksi}{36.0000\,ksi}}\right) = 0.9936$$

where f_v is determined as:

$$f_v = \frac{T}{2A_o t} \tag{44}$$

where

T = internal torque resulting from the factored loads, k-in.
A_o = enclosed area within the box section, in.^{2}
t = plate thickness

Equation 45 was used to find torque T

$$\tau_{max} = \frac{T t_{max}}{J} \tag{45}$$

Equation 45 was modified into the following

$$T = \frac{\tau_{max} J}{t_{max}} \tag{46}$$

where

τ_{max} = maximum shear calculated in the previous problems (kips)
J = torsional constant
t_{max} = maximum thickness within the cross section (in.)

where

$$J \approx \sum \frac{1}{3} b t^3 \tag{47}$$

$$\approx \sum\left(\frac{1}{3}\times 9.0000\times 0.7500^3\right)+\left(\frac{1}{3}\times 26.000\times 0.3750^3\right)$$
$$+\left(\frac{1}{3}\times 37.0000\times 0.4375^3\right)+\left(\frac{1}{3}\times 26.0000\times 0.3750^3\right)$$
$$+\left(\frac{1}{3}\times 8.0000\times 0.7500^3\right)+\left(\frac{1}{3}\times 4.0000\times 0.3750^3\right)=4.4078$$

$$T=\frac{(189.5400\,kips)(4.4078)}{0.7500\,in.}=1{,}113.9392\,K-in.$$

$$f_v=\frac{1{,}113.9392\,K-in.}{2.0000\times 23.7500\,in.\times 26.0000\,in.\times 0.3750\,in.}=2.4053\,ksi$$

$$F_n=(0.9936)(1.0000)(36.0000\,ksi)\sqrt{1.0000-3.0000\left(\frac{2.4053\,ksi}{36.0000\,ksi}\right)^2}=35.5293\,ksi$$

$$F_r=\phi_f F_n=(1.0000)(35.52931ksi)=35.5293\,ksi$$

$$M=F_r S_{xc} \tag{48}$$

$$M=(35.5293\,ksi)(452.2636\,in.^3)=16{,}068.6091\,in.-$$
$$=1{,}339.0508\ ft-kips$$

3. Negative flexure

Negative flexure was not considered because the stop logs are treated as simply supported beams.

Design shear strength

$$V_r=\phi_v V_n \tag{49}$$

where

V_r = factored shear resistance (kips)
ϕ_v = resistance factor for shear = 1.0000

V_n was determined by assuming $f_u = 0.75\phi_f F_y$

where F_y is the yield stress in ksi.

Therefore,

$$V_n = V_p \left[C + \frac{0.87(1-C)}{\sqrt{1+\left(\frac{d_o}{D}\right)^2}} \right] \tag{50}$$

where

V_p = plastic shear force (kips) = $0.5800 F_{yw} D t_w$ where D is web depth, in.
C = ratio of the shear buckling stress to the shear yield strength
d_o = stiffener spacing (in.)
F_{yw} = specified minimum yield strength of the web, ksi

$$V_p = (0.5800)(36.0000\,ksi)(26.0000\,in.)(0.3750\,in.) = 203.5800\,kips$$

The ratio C was determined

$$If \frac{D}{t_w} < 1.10\sqrt{\frac{EK}{F_{yw}}} \tag{51}$$

where K, the elastic buckling coefficient for shear strength, is calculated as

$$K = 5 + \frac{5}{\left(\frac{d_o}{D}\right)^2} \tag{52}$$

$$K = 5 + \frac{5}{\left(\frac{92.5625\,in.}{26.0000\,in.}\right)^2} = 5.3945$$

$$\frac{26.0000\,in.}{0.3750\,in.} < 1.10\sqrt{\frac{(29{,}000.0000\,ksi)(5.3944)}{36.0000\,ksi}}$$

$$69.333\overline{3} < 72.5124$$

therefore,

$$C = 1.0000$$

$$V_n = (203.5800\,kips)\left[1.0000 + \frac{0.8700(1.0000 - 1.0000)}{\sqrt{1.0000 + \left(\frac{92.5625\,in.}{26.0000\,in.}\right)^2}}\right] = 203.5800\,kips$$

$$V_r = \phi_f V_n = (1.0000)(203.5800) = 203.5800\,kips$$

The maximum uniform loads were determined using the minimum moment of 1,339.0493 ft-kips (compression flange) and shear of 203.5800 kips calculated using Equations 54 and 56.

$$M = \frac{wL^2}{8} \tag{53}$$

Equation 53 was modified as follows:

$$w_m = \frac{M \times 8}{L^2} \tag{54}$$

$$w_m = \frac{1,339.0508\,ft - kips \times 8.0000 \times 1000.0000\,lb}{25.0000^2\,ft^2} = 17,139.8502 lb\ /\ ft$$

$$V = \frac{w_s \times L}{2} \tag{55}$$

Equation 55 was modified as follows:

$$w_s = \frac{V \times 2}{L} \tag{56}$$

$$w_s = \frac{203.5800\,kips \times 2.0000 \times 1000.0000\,lb}{25.0000\ ft} = 16{,}286.4000\,lb\ /\ ft$$

The maximum pressure was determined using the minimum uniform load value between the moment and shear

$$P_c = \frac{w_m}{y} \tag{57}$$

where w is the minimum uniform load, lb/ft.

$$P_c = \frac{16{,}286.4000\,lb\ /\ ft}{3.1145\ ft} = 5{,}229.2181\,lb\ /\ ft^2$$

The maximum pressure height to reach a tension flange flexure failure is

$$h = \frac{P_c}{\gamma} \tag{58}$$

$$h = \frac{5{,}229.2181\,\frac{lb}{ft^2}}{62.4000\,\frac{lb}{ft^3}} = 83.8016\ ft$$

where h is the maximum height of stop log, ft.

3 Weld Capacity

The weld studied is a full-penetration groove weld. The capacity of the weld was determined for tension, compression, and shear, calculated according to Table J2.5 of AISC (2001).

The following calculations are for the weld capacity with the effective area for the skin plate shown in Figure 16 and use the following variables:

R = weld capacity, kips
ϕ = resistance factor = 0.9000
F_y = yield stress, ksi
A = area (in.^{2})

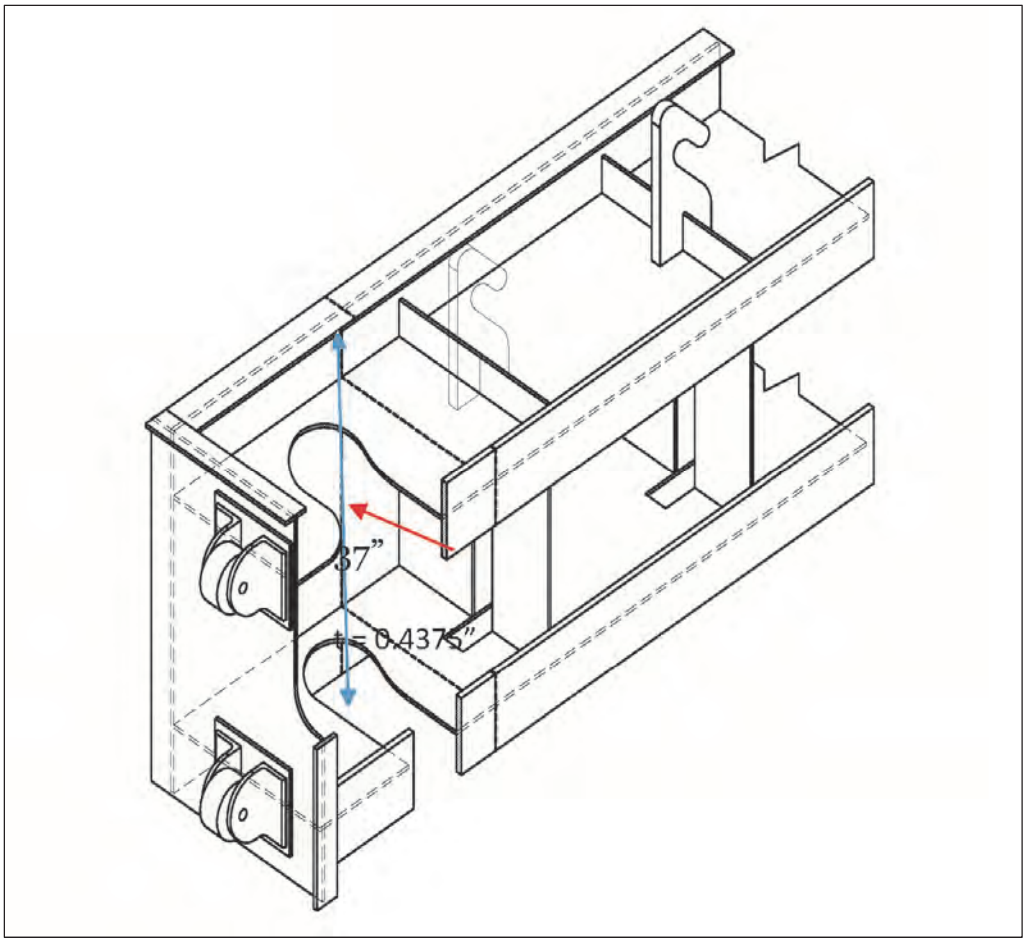

Figure 16. Indication of weld with effective area 16.18 in.^{2}. (furnished by USAED, Vicksburg).

- Tension

$$R = \phi F_y A = (0.90)(36\,ksi)(37\,in. \times 0.4375\,in.) = 542.4750\,kips$$

- Compression

$$R = \phi F_y A = (0.9)(36\,ksi)(37\,in. \times 0.4375\,in.) = 542.4750\,kips$$

- Shear

$$R = \phi F_y A = (0.9)(36\,ksi)(0.6)(37\,in. \times 0.4375\,in.) = 314.6850\,kips$$

The following calculations are for the weld capacity with the effective area of the webs as shown in Figure 17.

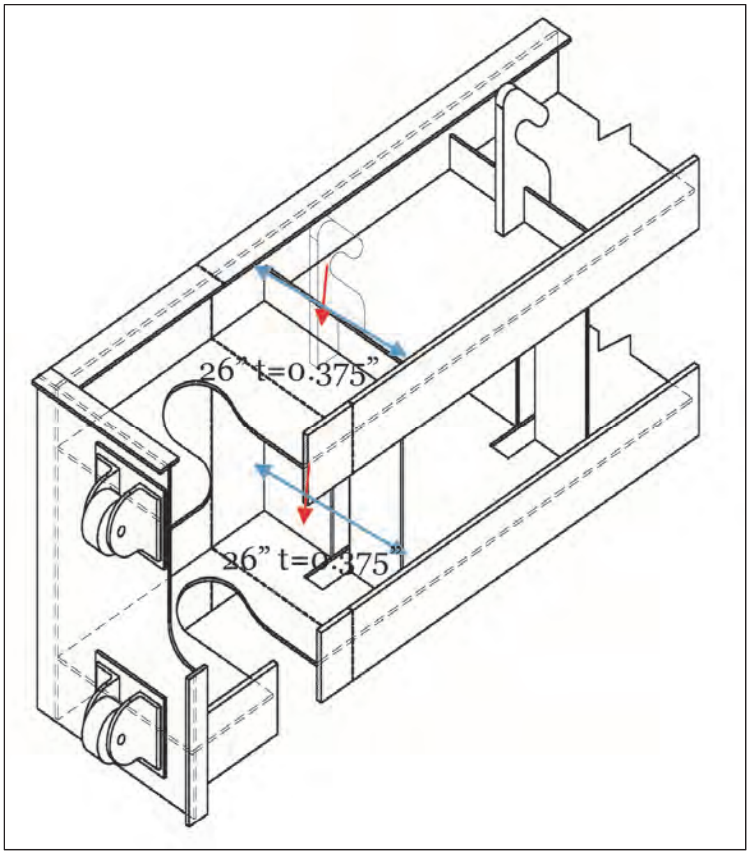

Figure 17. Indication of weld with effective area 9.75 in.² (furnished by USAED, Vicksburg).

- Tension

$$R = \phi F_y A = (0.90)(36\,ksi)(26\,in. \times 0.375\,in.) = 315.9000\,kips$$

- Compression

$$R = \phi F_y A = (0.9)(36\,ksi)(26\,in. \times 0.375\,in.) = 315.9000\,kips$$

- Shear

$$R = \phi F_y A = (0.9)(36\,ksi)(0.6)(26\,in. \times 0.375\,in.) = 189.5400\,kips$$

The following calculations are for the weld capacity with the effective area of the top flange shown in Figure 18.

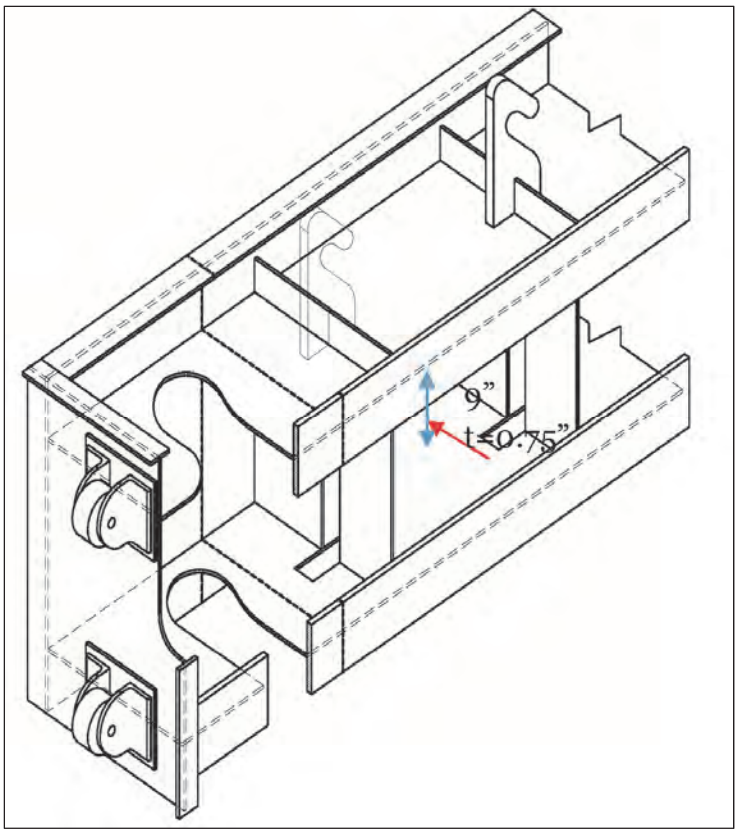

Figure 18. Indication of the weld effective area 6.75 in.^{2} (furnished by USAED, Vicksburg).

- Tension

$$R = \phi F_y A = (0.90)(36\,ksi)(9\,in. \times 0.75\,in.) = 218.7000\,kips$$

- Compression

$$R = \phi F_y A = (0.9)(36\,ksi)(9\,in. \times 0.75\,in.) = 218.7000\,kips$$

- Shear

$$R = \phi F_y A = (0.9)(36\,ksi)(0.6)(9\,in. \times 0.75\,in.) = 131.2200\,kips$$

The following calculations are for the weld capacity with the effective area of the bottom flange shown in Figure 19.

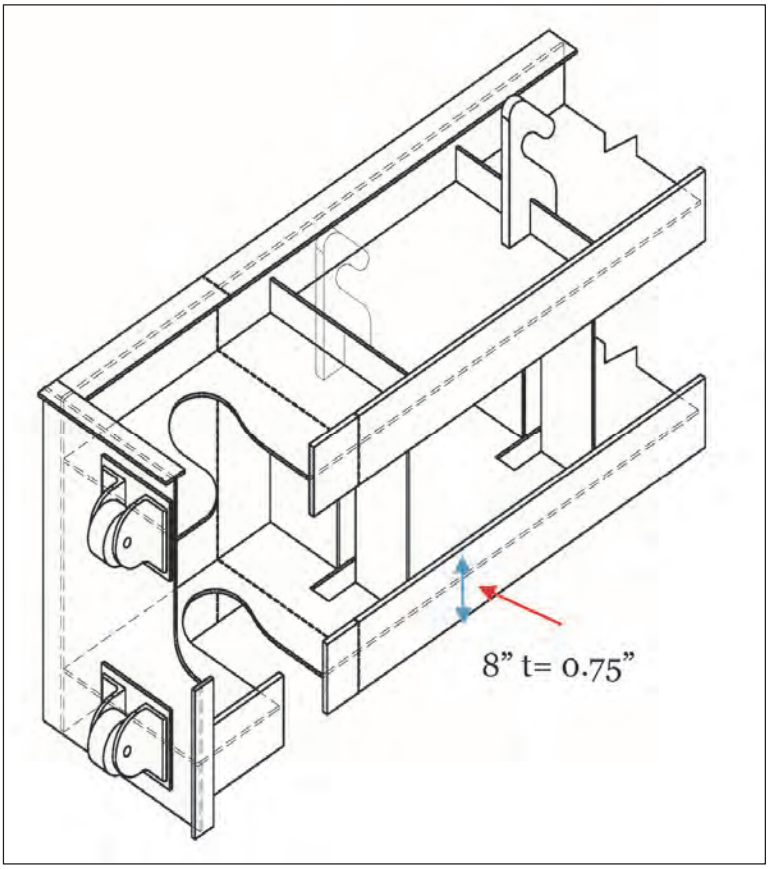

Figure 19. Indication of the weld with effective area 6 in.² (furnished by USAED, Vicksburg).

- Tension

$$R = \phi F_y A = (0.90)(36\,ksi)(8\,in. \times 0.75\,in.) = 194.4000\,kips$$

- Compression

$$R = \phi F_y A = (0.9)(36\,ksi)(8\,in. \times 0.75\,in.) = 194.4000\,kips$$

- Shear

$$R = \phi F_y A = (0.9)(36\,ksi)(0.6)(8\,in. \times 0.75\,in.) = 116.6400\,kips$$

The following calculations are for the weld capacity with the effective area of the skin plate flange shown in Figure 20.

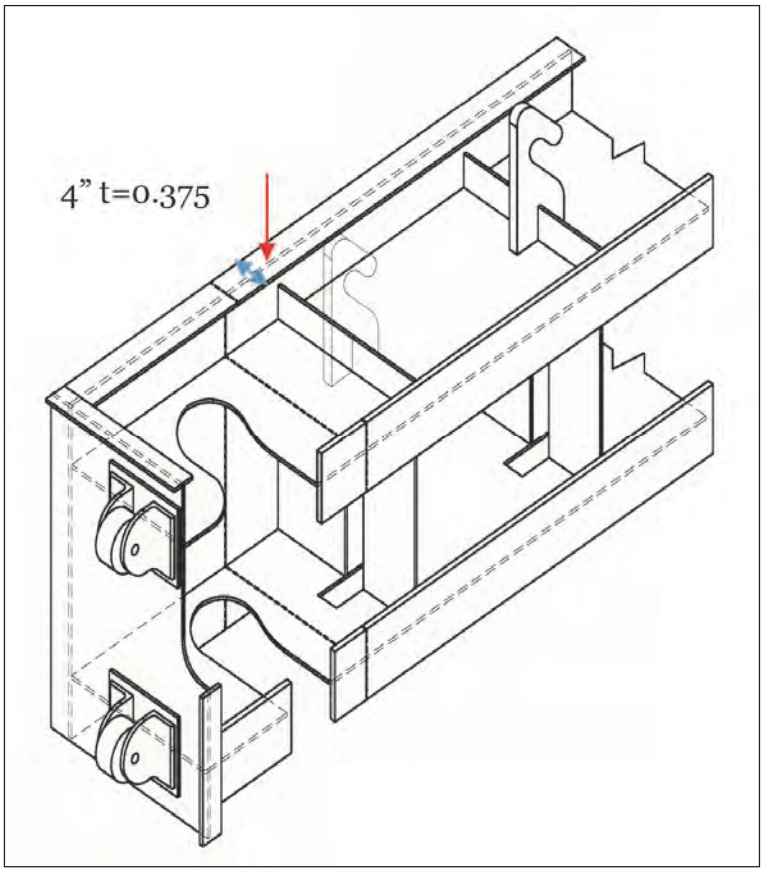

Figure 20. Indication of the weld with effective area 1.5 in.^{2} (furnished by USAED, Vicksburg)

- Tension

$$R = \phi F_y A = (0.90)(36\,ksi)(4\,in. \times 0.375\,in.) = 48.6000\,kips$$

- Compression

$$R = \phi F_y A = (0.9)(36\,ksi)(4\,in. \times 0.375\,in.) = 48.6000\,kips$$

- Shear

$$R = \phi F_y A = (0.9)(36\,ksi)(0.6)(4\,in. \times 0.375\,in.) = 29.1600\,kips$$

The weld capacity for the shear of the weld material will not be determined because the type of weld material is unknown.

4 Finite Element Analysis

Model description

This chapter presents a comprehensive three-dimensional finite element analysis conducted to assess the behavior of the stop log when submitted to the maximum pressures calculated analytically in Chapter 2. This analysis will provide the tools to validate the analytical solutions and provide the state of stresses on the cross section that will be welded. The three-dimensional model of the bottom stop log was developed using plate bending elements for all significant areas of the gate (Figure 21) and beam elements for the rollers. Figure 22 shows the uniform mesh used for the analysis. The model has 9837 nodes and 9825 shell elements with six degrees freedom per node.

Displacement and load boundary conditions

The displacement boundary conditions consisted of rollers on the bottom edge of the stop log restraining the movement in the z-z direction (Figure 23) assuming that the system was seated on the sill. The upstream-downstream direction (x-x) was restrained with rollers at the edge of the skin plate. To make the system stable, a series of springs along the direction of the gate were placed at the centerline locations of the rollers.

Figure 24 shows the force boundary conditions that consisted of the dead load and a uniform hydrostatic pressure of 33.0 psi (76.2 ft of head) in the positive y-y direction. The maximum hydrostatic pressure that produces the yield strength in the numerical model was determined using the maximum head calculated in Chapter 2, which corresponded to the box girder when a tension flange flexure failure occurs.

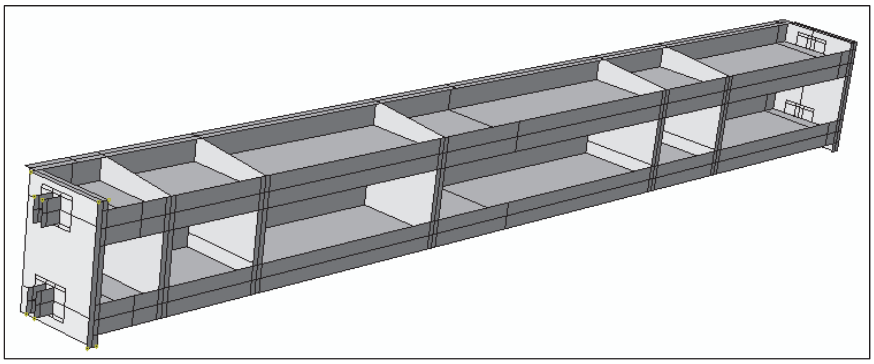

Figure 21. Geometrical model.

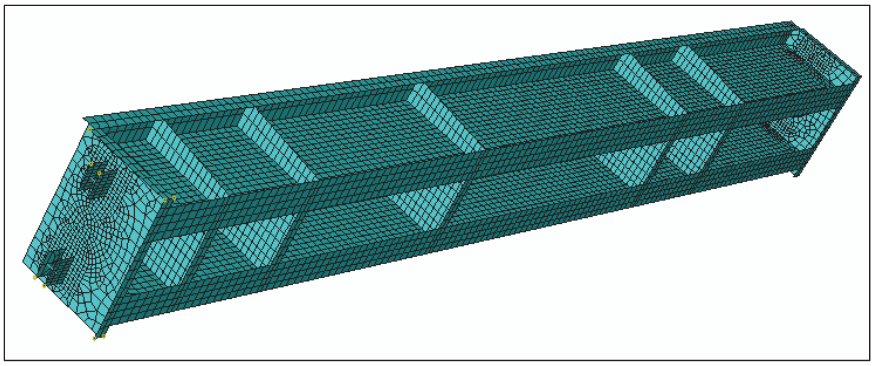

Figure 22. Finite element mesh.

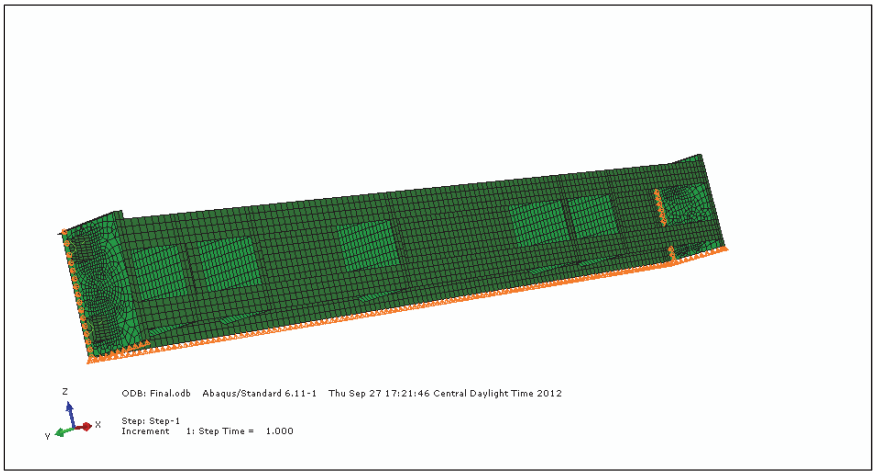

Figure 23. Displacement boundary conditions.

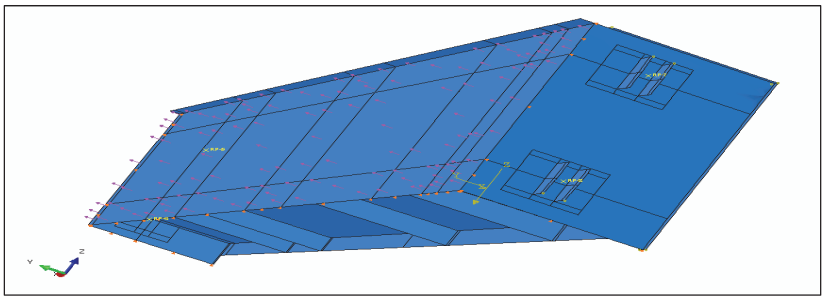

Figure 24. Force boundary conditions.

Results comparison with analytical solutions

The numerical model shows that the yield strength is reached at a head of 76.2 ft., while the analytical calculations showed 83.0 ft. of head, with just 8 percent of difference between the analytical and numerical solutions. The finite element analysis has a good correlation with the analytical solutions of the box girder. The 1-1 (x-x) direction is along the longitudinal axis of the gate, the 2-2 (y-y) direction is normal to the longitudinal

direction of the gate, and the 3-3 (z-z) direction goes along the elevation of the piers (Figure 24). Figure 25 shows the stresses in the 1-1 direction of the gate. The upstream side has a compression stress of 35.12 ksi, and the downstream side has a tension stress of 36.54 ksi. These results are also observed on the maximum and minimum principal stresses (Figures 26 and 27). They show that the gate is at the yield strength for a 76.2 ft of head.

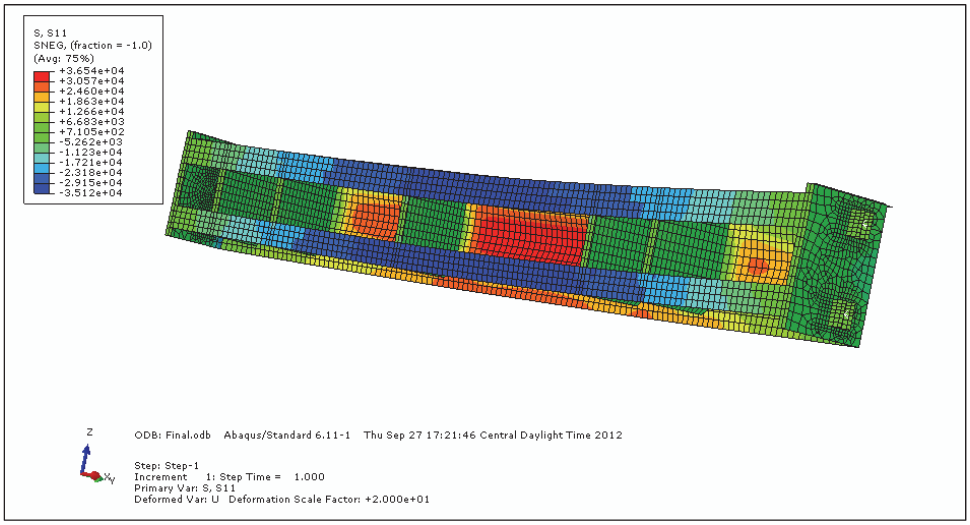

Figure 25. Stresses along longitudinal direction.

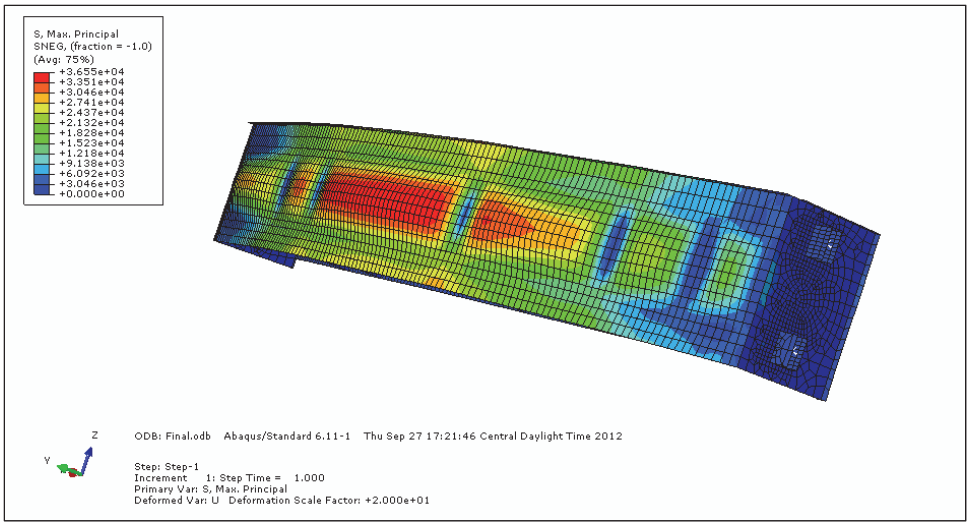

Figure 26. Maximum principal stresses.

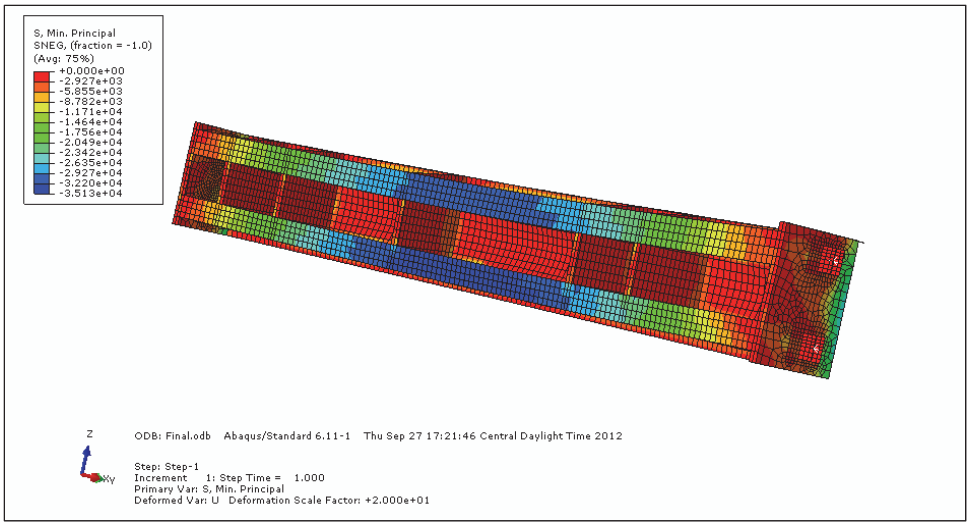

Figure 27. Minimum principal stresses.

5 Conclusions and Recommendations

Capacity calculations with the changes required to fit between the piers of the Little Sunflower Flood Control Drainage Structures' stop log were performed using the AISC (2001) and AASHTO (1998) criteria. The results show that the bridge criteria based on the box girder cross section provide the minimum capacity of 83.8 ft of head. The analytical results were compared with a finite element analysis, and they show an 8% difference between the analytical and numerical solution, therefore, it is a good correlation. The results for the different flexure and shear capacities for both methods (Table 9) show that the new stop log can resist 3.00 times the maximum elevation of the system. The welded connection capacities were also calculated, and the results are shown in Table 10 for tension, compression, and shear.

It is recommended that the welded connection be designed using a head of 83.0 ft. If failure occurs, it should occur in any location other than in the welded connection.

Table 9. The results of the flexural, shear, and maximum pressure.

Method	M_u	V_u	Max Pressure
Modified Section (w/effective width) (AISC (2001) LRFD)	$b_e = 4.72$: 482.5321 *ft-kips*	189.5400 *kips*	$6{,}323.7544\frac{lb}{ft^2}$
Box Girder (AASHTO (1998) LRFD)	1,339.0508 *ft-kips*	203.5800 *kips*	$5{,}229.2181\frac{lb}{ft^2}$

Table 10. The results of the capacity of the weld in tension, compression, and shear.

Effective Area, in.^{2}	Tension, kips	Compression, kips	Shear, kips
16.18	542.4750	542.4750	314.6850
9.75	315.9000	315.9000	189.5400
6.75	218.7000	218.7000	131.2200
6	194.4000	194.4000	116.6400
1.5	48.6000	48.6000	29.1600

References

American Association of State Highways and Transportation Officials. 1998. "Load and Resistance Factor Design (LRFD) Bridge Design Specifications," 2nd ed., Washington, DC.

American Institute of Steel Construction. 2001. "Manual of Steel Construction, Load and Resistance Factor Design (LRFD)," 3rd ed. Chicago, IL.

American Institute of Steel Construction. 2010. "Specification for Structural Steel Buildings," ANSI/AISC 360-10. Chicago, IL.

Headquarters, U.S. Army Corps of Engineers. 1994. *Structural Design of Closure Structures for Local Flood Protection Projects.* EM 1110-2-2705. Washington, DC.

Mississippi Levee Board. "Yazoo Backwater Pump Project." Accessed 8 May 2012 http://www.msleveeboard.com

Scott, Quinta. "Steele Bayou Drainage Structure." http://quintascott.wordpress.com, posted on May 31, 2011, Accessed 8 May 2012.

REPORT DOCUMENTATION PAGE

Form Approved
OMB No. 0704-0188

1. REPORT DATE *(DD-MM-YYYY)*	2. REPORT TYPE	3. DATES COVERED *(From - To)*
December 2012	Final	

4. TITLE AND SUBTITLE

Capacity Verification for Modifying Little Sunflower Flood Control Drainage Structure Stop Log

5a. CONTRACT NUMBER

5b. GRANT NUMBER

5c. PROGRAM ELEMENT NUMBER

6. AUTHOR(S)

Guillermo A. Riveros, DeAnna Dixon, and Elias Arredondo

5d. PROJECT NUMBER

5e. TASK NUMBER

5f. WORK UNIT NUMBER
9K76D4

7. PERFORMING ORGANIZATION NAME(S) AND ADDRESS(ES)

U.S. Army Engineer Research and Development Center
Information Technology Laboratory
3909 Halls Ferry Road, Vicksburg, MS 39180-6199

8. PERFORMING ORGANIZATION REPORT NUMBER

ERDC/ITL TR-12-5

9. SPONSORING / MONITORING AGENCY NAME(S) AND ADDRESS(ES)

U.S. Army Engineer District, Vicksburg
4155 Clay Street
Vicksburg, MS 39183

10. SPONSOR/MONITOR'S ACRONYM(S)

11. SPONSOR/MONITOR'S REPORT NUMBER(S)

12. DISTRIBUTION / AVAILABILITY STATEMENT

Approved for public release; distribution is unlimited.

13. SUPPLEMENTARY NOTES

14. ABSTRACT

The Steel Bayou and Little Sunflower Flood Control Drainage Structures are the two drainage structures of the Yazoo Backwater Project. They were completed in 1969 and 1975, respectively. The structures allow the storm water of the Mississippi Delta to pass through the open vertical lift gates into the Mississippi/Yazoo River when stages on the riverside of the levees are lower than the stages on the interior basin. When the stages of the Mississippi/Yazoo River are higher than the stages of the interior basin, the vertical lift gates are closed, keeping floodwaters from backing up into the South Delta. The Steel Bayou Drainage Structure is located 0.75 mile north of the Yazoo River mile 9.7 and has four vertical lift gates 23.5 ft high and 31 ft wide. The Little Sunflower Drainage Structure is located north of the Yazoo River at mile 32.6 and has two vertical lift gates 25 ft wide and 22.5 ft high.

This report presents analytical and numerical calculations for the modification of the Steel Bayou stop logs to be used permanently at the Little Sunflower project. The calculations were conducted using the approach used to design miter gates horizontal girders using the 2001 criteria of the American Institute of Steel Construction (AISC) and the box girder calculations from the American Association of State Highways and Transportation Officials Load and Resistance Factor Design (LRFD) bridge manual.

15. SUBJECT TERMS

Little Sunflower Drainage Structure
Stop log
Stop log modification
Verification of Little Sunflower Drainage Structure
Weld capacity

16. SECURITY CLASSIFICATION OF:			17. LIMITATION OF ABSTRACT	18. NUMBER OF PAGES	19a. NAME OF RESPONSIBLE PERSON
a. REPORT	b. ABSTRACT	c. THIS PAGE			19b. TELEPHONE NUMBER *(include area code)*
UNCLASSIFIED	UNCLASSIFIED	UNCLASSIFIED		55	